Supplementary information

Global land carbon sink response to temperature and precipitation varies with ENSO phase

Yuanyuan Fang, Anna M. Michalak, Christopher R. Schwalm, Deborah N. Huntzinger, Joseph A. Berry, Philippe Ciais, Shilong Piao, Benjamin Poulter, Josh B. Fisher, Robert B. Cook, Daniel Hayes, Maoyi Huang, Akihiko Ito, Atul Jain, Huimin Lei, Chaoqun Lu, Jiafu Mao, Nicholas C. Parazoo, Shushi Peng, Daniel M. Ricciuto, Xiaoying Shi, Bo Tao, Hanqin Tian, Weile Wang, Yaxing Wei, Jia Yang

Supplementary text

1. Tropical terrestrial ecosystems drive the phase-dependent response of atmospheric CO_2 growth rate (AGR) to ENSO

The variations in the growth rate of atmospheric CO_2 concentrations are possibly driven by many processes, including changes in fossil fuel emissions, land use and land cover, fire emissions, ocean sink and the terrestrial ecosystem. We find, however, on the interannual scale, the response of AGR to tropical precipitation (TMAP) and tropical temperature (TMAT) is mainly driven by the tropical terrestrial ecosystem.

Our conclusion is based on analyses on the interannual variances, temperature and precipitation correlations, as well as ENSO responses of each component contributing to AGR, including fossil fuel emissions from CDIAC, GCP-CICERO, UNFCCC(Boden et al., 2013), ocean sink from multiple biogeochemical and transport ocean models, and two observation-based estimates(Le Quéré et al., 2014), emissions due to land use land cover change(Houghton et al., 2012), and the residual land sink (RLS)(Le Quéré et al., 2015) (all obtained from the Global Carbon Project, GCP), as well as CO_2 fire emissions from GFED4.1s (based on an updated version of van der Werf et al.(van der Werf et al., 2010) with both the standard GFED4 burned area(Giglio et al., 2013) and the small fire burned area(Randerson et al., 2012)). The interannual variances of those components and the partial correlations of those components with tropical temperature and precipitation are estimated after detrending their annual time series.

We find that, first, that the interannual variability in fossil fuel emissions(Boden et al., 2013), land use change(Houghton et al., 2012), ocean CO_2 uptake(Le Quéré et al., 2014), and fire emissions(Giglio et al., 2013; Randerson et al., 2012; van der Werf et al., 2010) is small relative to the the interannual variability in AGR(Wang et al., 2013). The variance of the interannual variability of CO_2 fluxes from detrended fossil fuel combustion, land use change, and oceanic CO_2 uptake based on GCP estimates(Le Quéré et al., 2015) is 0.09, 0.03, and 0.05 $(Pg\ C\ yr^{-1})^2$, respectively, each accounting for less

than 10% of the variability in the AGR of a variance of 0.95 (Pg C yr^{-1})^2. Estimates of fire emissions are not available for the full period examined here, but the variance across a shorter period (1997-2010) based on GFED4.1s estimates is also low (0.08 Pg C yr^{-1})(Giglio et al., 2013) relative to that of AGR. Second, the interannual variability in these other flux components does not correlate with TMAT and TMAP in a manner consistent with AGR (Fig. S9). Namely, fire emissions are positively correlated with TMAT across all ENSO phases, and none of the other components exhibit a significant correlation with TMAT under any ENSO conditions, whereas the relationship between AGR and TMAT is phase-dependent. For TMAP, fossil fuel emissions following El Niño conditions and ocean fluxes across all years show correlations, but the sign of these correlations is opposite from AGR, and the phase dependence is also inconsistent. In addition, the correlation between fossil fuel emissions and TMAP is suspect, both because there is no clear mechanistic explanation for such a correlation. Finally, an analysis substituting the CO_2 Residual Land Sink (RLS) for AGR (Methods)(Le Quéré et al., 2015) shows that conclusions regarding temperature response are consistent with those based on the AGR analysis (Fig. S10). The relationship with TMAP is consistent with AGR post La Niña and for all years, while an inconsistency occurring post El Niño is driven by two years with extreme low (1987) and high (2010) tropical precipitation. RLS seems to be affected by those extreme precipitation years more than AGR, however, when examining each individual component used to estimate RLS, we find that such sensitivity of RLS to extreme precipitation results from the suspicious observed correlation between fossil fuel CO_2 emissions and precipitation (Fig. S10).

Overall, these facts support the conclusion that tropical land ecosystems drive the ENSO-dependent responses of AGR to temperature and precipitation because we find that AGR is insignificantly and weakly correlated with climatic drivers either in Northern or Southern extra tropics ($|r|$ never exceeds 0.4 across all ENSO phases). This conclusion is consistent with literature that show ecosystems in tropics dominates the interannual variability in global land sink while the extratropical ecosystem has a much

weaker and delayed response to climate variability in temperature or precipitation (Baker et al., 2006; Braswell et al., 1997; Le Quere et al., 2009; Sitch et al., 2008; VukiĆEviĆ et al., 2001).

2. The phase-dependent response of AGR to ENSO is not driven by a few extreme years

We conducted a number of sensitivity analyses to examine the possibility that a few extreme events may contribute to the observed phase-dependent response of AGR to ENSO. The extremes we tested include the anomalously strong El Niño events during 1997-1998, European drought during 2003, and Russian drought in 2010. Our main conclusion remains unchanged even when excluding those years from our analyses, suggesting that the phase-dependency of AGR response to ENSO is not driven by a few extreme events.

3. More persistent La Niña does not account for the significant correlation between AGR and tropical precipitation post La Niña

One key difference between El Niño and La Niña events is that La Niña events tend to be more persistent (Okumura and Deser, 2010). However, we find that such nature of La Niña does not explain the significant negative correlation between AGR and tropical precipitation. We do see that while a majority of post El Niño years are either an individual year or two consecutive years, post La Niña years may include three consecutive years. Such results are consistent with the fact that La Niña events often last longer than El Niño years. However, when excluding all third consecutive post La Niña years from our analysis, we find similar significant negative correlations between AGR and tropical precipitation. This sensitivity analysis thus suggests that the strong negative correlation between tropical precipitation and AGR post La Niña is unlikely related to the fact that La Niña is more persistent that El Niño.

Supplementary tables

Table S1: 10 Terrestrial Biospheric Models are provided by the Multi-scale Synthesis and Terrestrial Model Intercomparison Project (MsTMIP) and used in this study. Carbon flux data, including Net Ecosystem Exchange (NEE), Gross Primary Production (GPP), Total Respiration (TRE), are in the output of those models bundled as the MsTMIP 1.0 data release(Huntzinger et al., 2014).

	Model	References
With dynamical N-cycle	BIOME-BGC	(Thornton et al., 2002)
	CLM4	(Mao et al., 2012) and (Oleson et al., 2010)
	CLM4VIC	(Lei et al., 2014)
	DLEM	(Tian et al., 2012)
	ISAM	(Barman et al., 2014a, b; Jain et al., 2009)
Without dynamical N-cycle	GTEC	(King et al., 1997) and (Ricciuto et al., 2011)
	LPJ-wsl	(Sitch et al., 2003)
	ORCHIDEE-LSCE	(Krinner et al., 2005)
	VEGAS	(Zeng et al., 2005)
	VISIT	(Ito, 2010)

Supplementary figures

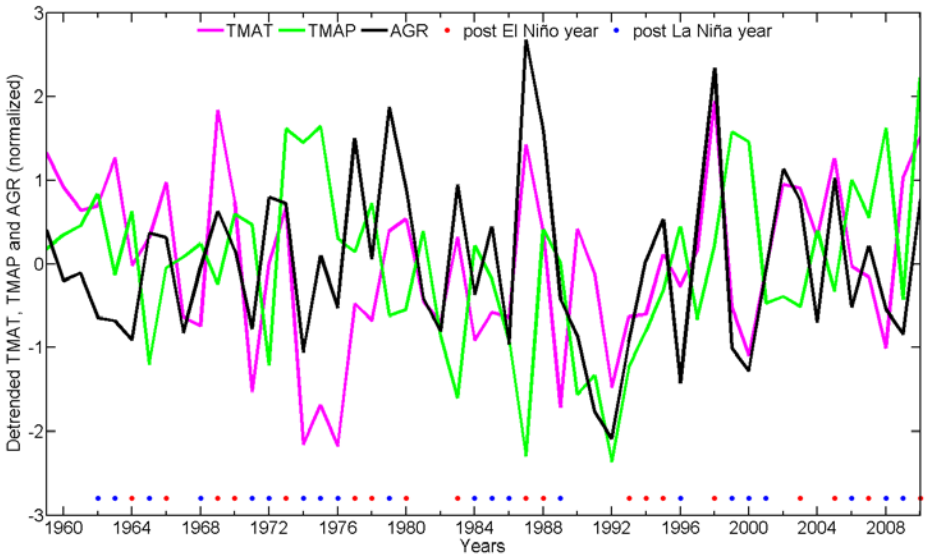

Figure S1. Timeseries of detrended annual AGR (black), TMAT (magenta) and TMAP (green) (Normalized). Blue and red dots mark post El Niño and post La Niña years.

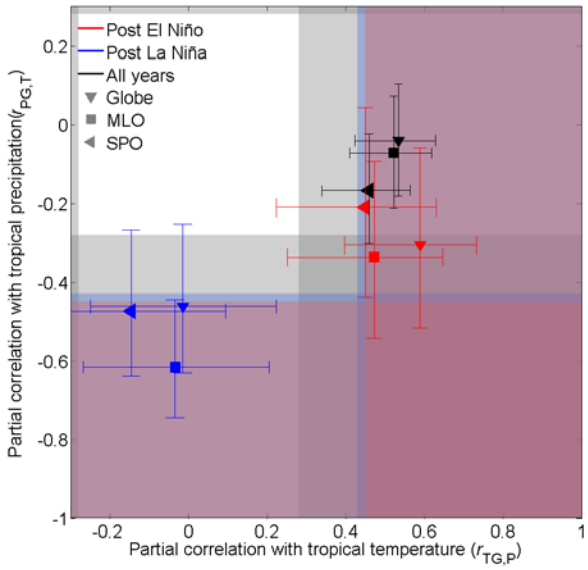

Figure S2. The phase-dependent response of AGR to tropical temperature and precipitation is robust in spite of the metrics and data applied to estimate AGR. Similar to Fig 1., but AGR is estimated as the differences of atmospheric CO_2 data of January averages of Mauna Loa (MLO) and South Pole (SPO) mean (Downward pointing triangles), MLO only (squares) and SPO only (left-pointing triangles).

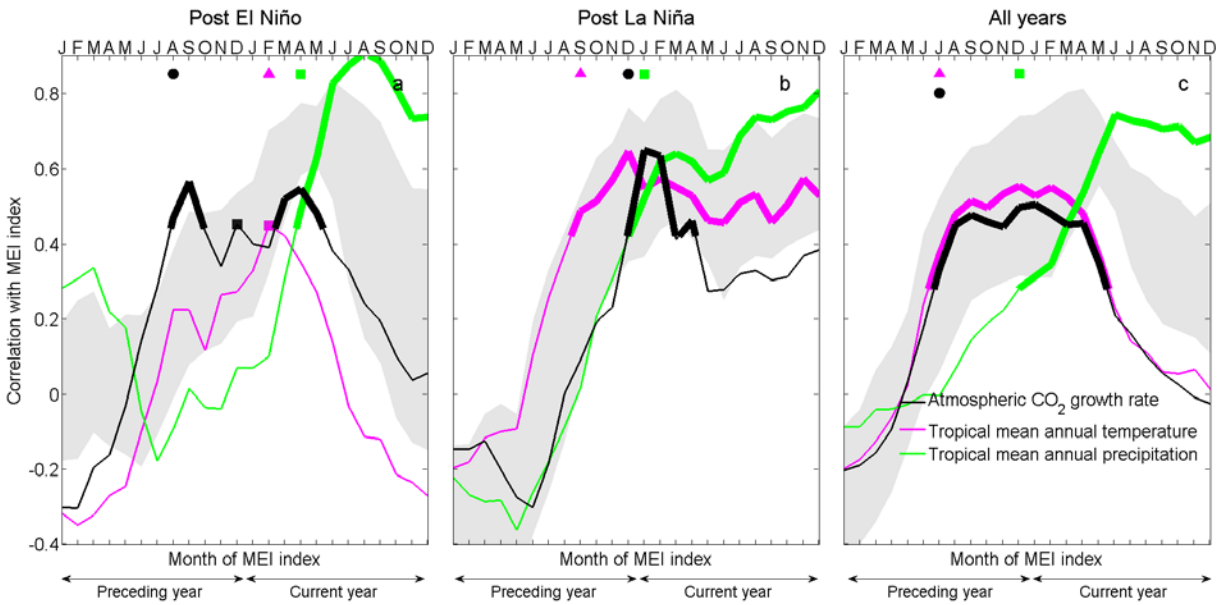

99

100 **Figure S3.** The phase-dependent response of AGR to ENSO indices is robust in spite of the choice of

101 ENSO index. Similar to Fig. 2, but using MEI instead of Niño 3.4.

102

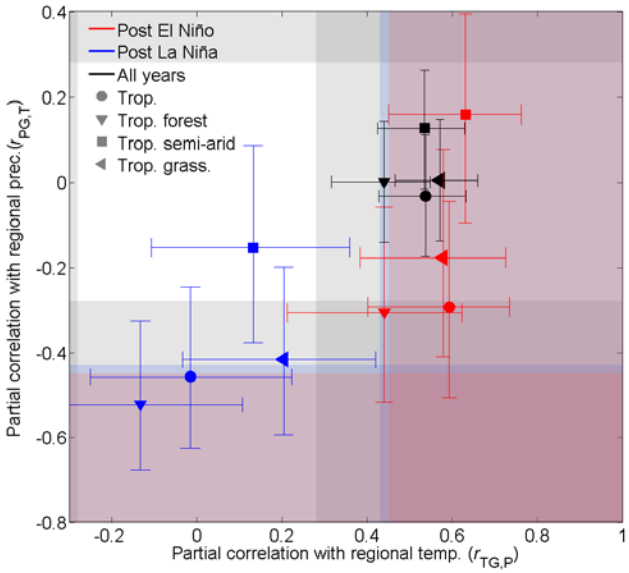

103

104 **Figure S4:** Similar to Fig. 1, but showing AGR vs. temperature and precipitation over tropical land
105 (circles), tropical forests (downward-pointing triangles), tropical semi-arid areas (squares) and tropical
106 grassland and crops (left-pointing triangles).

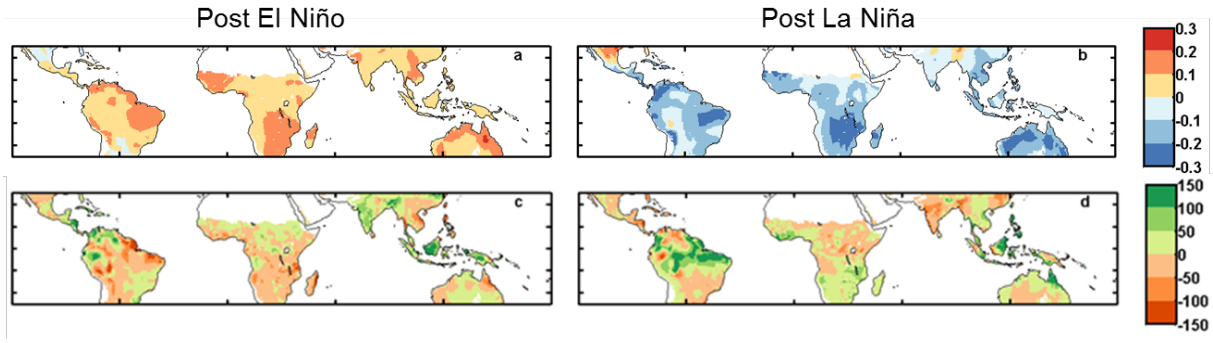

Figure S5: Tropical areas are hotter and drier post El Niño than post La Niña. Spatial distribution of (a, b) temperature (unit: k) and (c, d) precipitation (unit: mm yr^{-1}) anomalies (a, c) post El Niño and (b, d) post La Niña.

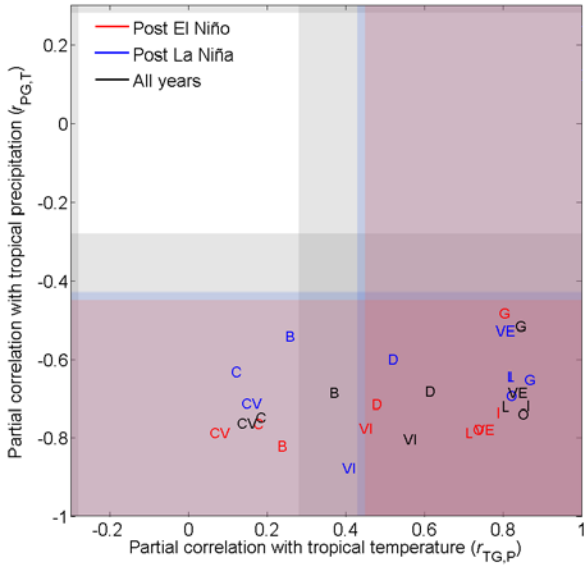

Figure S6: None of MsTMIP models simulates the phase-dependent response of tropical NEE to tropical temperature and precipitation consistent with that observed from the AGR. Similar to Fig. 1, but each group of capital letters represents the partial correlations between detrended anomalies of tropical NEE as simulated by 10 individual terrestrial biospheric model and TMAT (TMAP) while controlling TMAP(TMAT), with B: BIOME-BGC; C: CLM4; CV: CLM4VIC; D: DLEM; G: GTEC; I: ISAM; L: LPJ-wsl; O: ORCHIDEE-LSCE; VE: VEGAS; VI: VISIT.

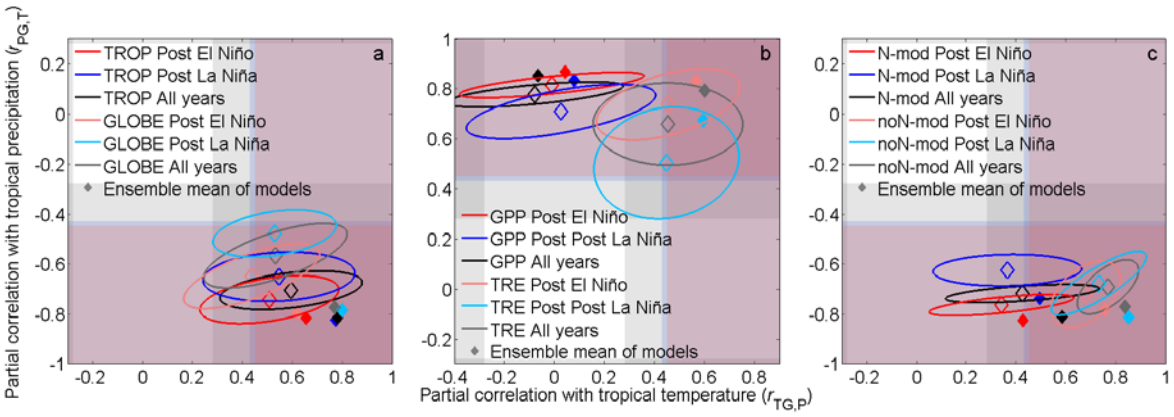

Figure S7: The responses of carbon fluxes to tropical temperature and precipitation inferred from simulations. (a) Simulated global NEE correlations with temperature and precipitation appear similar to that of tropical NEE. Diamonds show partial correlations between detrended anomalies of global NEE and TMAT (TMAP) while controlling TMAP (TMAT) for all (dark gray), post El Niño (light coral) and post La Niña years (light sky blue) estimated using ensemble mean of 10 models, in comparison to corresponding results of tropical NEE for all (black), post El Niño (red) and post La Niña years (blue). (b) Simulated tropical GPP and TRE correlations to precipitation are strong under all ENSO conditions. Diamonds show the partial correlations between detrended anomalies of tropical GPP and TMAT (TMAP) while controlling TMAP (TMAT), estimated using ensemble mean of 10 models for all (black), post El Niño (red) and post La Niña years (blue), in conjunction with corresponding results of tropical TRE for all (dark gray), post El Niño (light coral) and post La Niña years (light sky blue). (c) Simulated tropical NEE correlations to temperature and precipitation are not improved by models with interactive nitrogen. Diamonds show the partial correlations between detrended anomalies of tropical NEE and TMAT (TMAP) while controlling TMAP (TMAT), estimated using ensemble mean of 5 models with interactive nitrogen for all (black), post El Niño (red) and post La Niña years (blue) in comparison with corresponding results estimated using ensemble mean of 6 models without interactive nitrogen for all (dark gray), post El Niño (light coral) and post La Niña years (light sky blue). Ellipses depict contour lines of 1 standard deviation of the bivariate Gaussian distribution fitted to the partial correlations with TMAT/with TMAP as estimated from corresponding individual models with empty diamonds inside indicating the mean values of those partial correlations. The shaded area indicates the critical values of partial correlations as in Fig. 1.

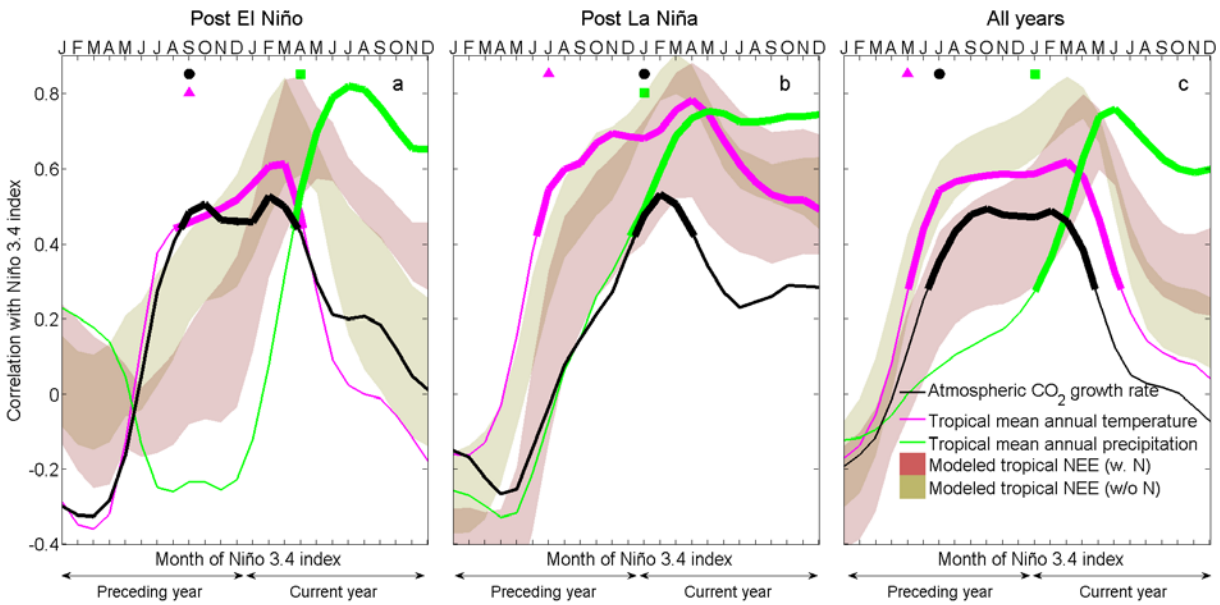

Figure S8: Models do not reproduce the different timing of AGR responses to ENSO no matter if they include dynamical nitrogen cycle. Similar to Fig. 2, but models are shown in two groups (with dynamical N-cycle, brownish shade and without dynamical N-cycle, greenish shade, see Table S1 for models that fall into each category).

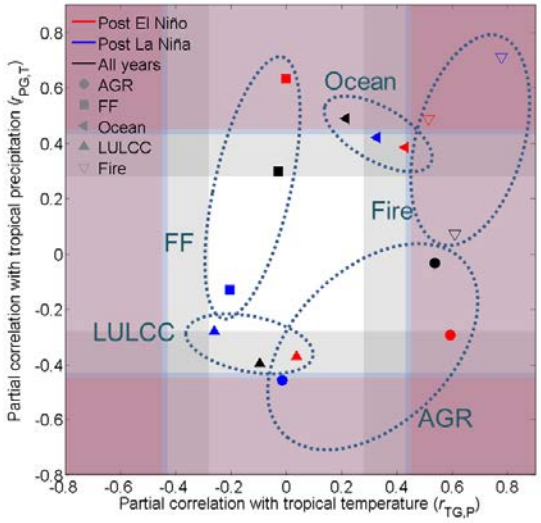

147

148 **Figure S9:** Correlations of fossil fuel (FF), land use land cover change (LULCC), ocean (Ocean) and fire
149 emission components to tropical mean annual temperature (TMAT) and precipitation (TMAP) does not
150 show differences across ENSO phases consistently as in AGR. The sign of each component is adjusted so
151 that a positive value indicates releasing CO_2 to the atmosphere. Symbols represent partial correlations
152 between detrended anomalies of AGR and TMAT, and between detrended anomalies of AGR and TMAP,
153 while controlling for the third variable. Filled circles represent AGR estimated using NOAA ESRL
154 measurements while filled squares, left-pointing triangles and downward-pointing triangles represent CO_2
155 released by fossil fuel combustion(Boden et al., 2013), ocean(Le Quéré et al., 2014) and land use land
156 cover change(Houghton et al., 2012) estimated by the Global Carbon Project(Le Quéré et al., 2015). For
157 all AGR and its components except fire emissions, correlations are calculated over the period 1959-2010,
158 with black representing all years, red indicating post El Niño conditions, and blue indicating post La Niña
159 conditions. The pink, blue and grey shaded area delineates the range for significant partial correlations
160 (p<0.05) for post El Niño ($|r|$>0.46), post La Niña ($|r|$>0.44), all year cases ($|r|$>0.28) using a two-tailed
161 tests for all emission components (filled symbols) except fire emissions (empty symbols). Fire emissions
162 are from GFED4.1s inventory(Giglio et al., 2013; Randerson et al., 2012; van der Werf et al., 2010),
163 covering the time period of 1997-2010 (14 years in total, including 5 post El Niño years and 6 post La
164 Niña years). Due to the short time period of those fire emissions, their estimated partial correlations to
165 tropical temperature and tropical precipitation are all insignificant except for the all year case for tropical
166 temperature. Dashed ellipses are used to highlight the groups of all-year, post El Nino and post La Nina
167 correlations as estimated for AGR and each of the AGR components, including CO_2 released by FF,
168 LULCC, Ocean, and Fires.

169

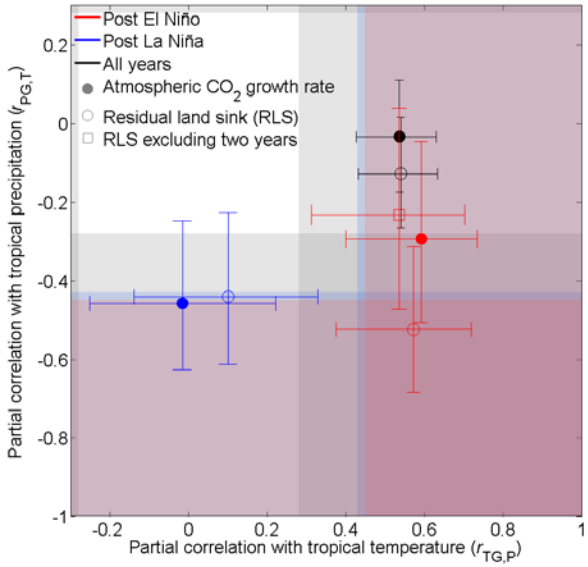

170

171 **Figure S10:** Similar to Fig. 1, but in addition to AGR (filled circles), also plotted in the figure is Residual
172 land sink (empty circles). For post El Niño years, residual land sink is also plotted by excluding 1987 and
173 2010 from the partial correlation analysis (empty squares).

174

175

176

177 References

178

179 Baker, D. F., Law, R. M., Gurney, K. R., Rayner, P., Peylin, P., Denning, A. S., Bousquet, P., Bruhwiler,
180 L., Chen, Y. H., Ciais, P., Fung, I. Y., Heimann, M., John, J., Maki, T., Maksyutov, S., Masarie, K.,
181 Prather, M., Pak, B., Taguchi, S., and Zhu, Z.: TransCom 3 inversion intercomparison: Impact of
182 transport model errors on the interannual variability of regional CO2 fluxes, 1988–2003, Global
183 Biogeochemical Cycles, 20, GB1002, 2006.

184 Barman, R., Jain, A. K., and Liang, M.: Climate-driven uncertainties in modeling terrestrial energy and
185 water fluxes: a site-level to global-scale analysis, Global Change Biology, 20, 1885-1900, 2014a.

186 Barman, R., Jain, A. K., and Liang, M.: Climate-driven uncertainties in modeling terrestrial gross primary
187 production: a site level to global-scale analysis, Global Change Biology, 20, 1394-1411, 2014b.

188 Boden, T. A., Marland, G., and Andres, R. J.: Global, Regional, and National Fossil-Fuel CO2 Emissions,
189 Carbon Dioxide Information Analysis Center, Oak Ridge National Laboratory, U.S. Department of
190 Energy, Oak Ridge, Tenn., U.S.A., doi: 10.3334/CDIAC/00001_V2010, 2013. 2013.

191 Braswell, B. H., Schimel, D. S., Linder, E., and Moore, B.: The Response of Global Terrestrial
192 Ecosystems to Interannual Temperature Variability, Science, 278, 870-873, 1997.

193 Giglio, L., Randerson, J. T., and Van Der Werf, G. R.: Analysis of daily, monthly, and annual burned area
194 using the fourth-generation global fire emissions database (GFED4), Journal of Geophysical Research:
195 Biogeosciences, 118, 317-328, 2013.

196 Houghton, R. A., House, J. I., Pongratz, J., Van Der Werf, G. R., Defries, R. S., Hansen, M. C., Le Quéré,
197 C., and Ramankutty, N.: Carbon emissions from land use and land-cover change, Biogeosciences, 9,
198 5125-5142, 2012.

199 Huntzinger, D., Schwalm, C. R., Y. Wei, R.B. Cook, A.M. Michalak, K. Schaefer, A.R. Jacobson, M.A.
200 Arain, P. Ciais, J.B. Fisher, D.J. Hayes, M. Huang, S. Huang, A. Ito, A.K. Jain, H. Lei, C. Lu, F.
201 Maignan, J. Mao, N. Parazoo, C. Peng, S. Peng, B. Poulter, D.M. Ricciuto, H. Tian, Xiaoying Shi, W.
202 Wang, N. Zeng, and F. Zhao, A. Q. Z.: NACP MsTMIP: Global 0.5-deg Terrestrial Biosphere Model
203 Outputs (version 1) in Standard Format, Oak Ridge National Laboratory Distributed Active Archive
204 Center, Oak Ridge, Tennessee, USA., doi: 10.3334/ORNLDAAC/1225., 2014. 2014.

205 Ito, A.: Changing ecophysiological processes and carbon budget in East Asian ecosystems under near-
206 future changes in climate: implications for long-term monitoring from a process-based model, J Plant Res,
207 123, 577-588, 2010.

208 Jain, A., Yang, X., Kheshgi, H., Mcguire, A. D., Post, W., and Kicklighter, D.: Nitrogen attenuation of
209 terrestrial carbon cycle response to global environmental factors, Global Biogeochemical Cycles, 23,
210 2009.

211 King, A. W., Post, W. M., and Wullschleger, S. D.: The potential response of terrestrial carbon storage to
212 changes in climate and atmospheric CO2, Climatic Change, 35, 199-227, 1997.

Krinner, G., Viovy, N., De Noblet-Ducoudré, N., Ogée, J., Polcher, J., Friedlingstein, P., Ciais, P., Sitch, S., and Prentice, I. C.: A dynamic global vegetation model for studies of the coupled atmosphere-biosphere system, Global Biogeochemical Cycles, 19, GB1015, 2005.

Le Quéré, C., Moriarty, R., Andrew, R. M., Peters, G. P., Ciais, P., Friedlingstein, P., Jones, S. D., Sitch, S., Tans, P., Arneth, A., Boden, T. A., Bopp, L., Bozec, Y., Canadell, J. G., Chini, L. P., Chevallier, F., Cosca, C. E., Harris, I., Hoppema, M., Houghton, R. A., House, J. I., Jain, A. K., Johannessen, T., Kato, E., Keeling, R. F., Kitidis, V., Klein Goldewijk, K., Koven, C., Landa, C. S., Landschützer, P., Lenton, A., Lima, I. D., Marland, G., Mathis, J. T., Metzl, N., Nojiri, Y., Olsen, A., Ono, T., Peng, S., Peters, W., Pfeil, B., Poulter, B., Raupach, M. R., Regnier, P., Rödenbeck, C., Saito, S., Salisbury, J. E., Schuster, U., Schwinger, J., Séférian, R., Segschneider, J., Steinhoff, T., Stocker, B. D., Sutton, A. J., Takahashi, T., Tilbrook, B., Van Der Werf, G. R., Viovy, N., Wang, Y. P., Wanninkhof, R., Wiltshire, A., and Zeng, N.: Global carbon budget 2014, Earth Syst. Sci. Data, 7, 47-85, 2015.

Le Quéré, C., Peters, G. P., Andres, R. J., Andrew, R. M., Boden, T. A., Ciais, P., Friedlingstein, P., Houghton, R. A., Marland, G., Moriarty, R., Sitch, S., Tans, P., Arneth, A., Arvanitis, A., Bakker, D. C. E., Bopp, L., Canadell, J. G., Chini, L. P., Doney, S. C., Harper, A., Harris, I., House, J. I., Jain, A. K., Jones, S. D., Kato, E., Keeling, R. F., Klein Goldewijk, K., Körtzinger, A., Koven, C., Lefèvre, N., Maignan, F., Omar, A., Ono, T., Park, G. H., Pfeil, B., Poulter, B., Raupach, M. R., Regnier, P., Rödenbeck, C., Saito, S., Schwinger, J., Segschneider, J., Stocker, B. D., Takahashi, T., Tilbrook, B., Van Heuven, S., Viovy, N., Wanninkhof, R., Wiltshire, A., and Zaehle, S.: Global carbon budget 2013, Earth Syst. Sci. Data, 6, 235-263, 2014.

Le Quere, C., Raupach, M. R., Canadell, J. G., Marland, G., and Et Al.: Trends in the sources and sinks of carbon dioxide, Nature Geosci, 2, 831-836, 2009.

Lei, H., Huang, M., Leung, L. R., Yang, D., Shi, X., Mao, J., Hayes, D. J., Schwalm, C. R., Wei, Y., and Liu, S.: Sensitivity of global terrestrial gross primary production to hydrologic states simulated by the Community Land Model using two runoff parameterizations, Journal of Advances in Modeling Earth Systems, 6, 658-679, 2014.

Mao, J., Thornton, P. E., Shi, X., Zhao, M., and Post, W. M.: Remote Sensing Evaluation of CLM4 GPP for the Period 2000–09, Journal of Climate, 25, 5327-5342, 2012.

Okumura, Y. M. and Deser, C.: Asymmetry in the Duration of El Niño and La Niña, Journal of Climate, 23, 5826-5843, 2010.

Oleson, K. W., Lawrence, D. M., Gordon, B., Flanner, M. G., Kluzek, E., Peter, J., Levis, S., Swenson, S. C., Thornton, E., Feddema, J., and Others: Technical description of version 4.0 of the Community Land Model (CLM), doi: 10.5065/D6FB50WZ, 2010.

Randerson, J. T., Chen, Y., Van Der Werf, G. R., Rogers, B. M., and Morton, D. C.: Global burned area and biomass burning emissions from small fires, Journal of Geophysical Research: Biogeosciences, 117, 2012.

Ricciuto, D. M., King, A. W., Dragoni, D., and Post, W. M.: Parameter and prediction uncertainty in an optimized terrestrial carbon cycle model: Effects of constraining variables and data record length, Journal of Geophysical Research: Biogeosciences, 116, 2011.

Sitch, S., Huntingford, C., Gedney, N., Levy, P. E., Lomas, M., Piao, S. L., Betts, R., Ciais, P., Cox, P., Friedlingstein, P., Jones, C. D., Prentice, I. C., and Woodward, F. I.: Evaluation of the terrestrial carbon cycle, future plant geography and climate-carbon cycle feedbacks using five Dynamic Global Vegetation Models (DGVMs), Global Change Biology, 14, 2015-2039, 2008.

Sitch, S., Smith, B., Prentice, I., Arneth, A., Bondeau, A., Cramer, W., Kaplan, J., Levis, S., Lucht, W., Sykes, M., Thonicke, K., and Venevsky, S.: Evaluation of ecosystem dynamics, plant geography and terrestial carbon cycling in the LPJ dynamic global vegetation model, Global Change Biology, 9, 161 - 185, 2003.

Thornton, P. E., Law, B. E., Gholz, H. L., Clark, K. L., Falge, E., Ellsworth, D. S., Golstein, A. H., Monson, R. K., Hollinger, D., Falk, M., Chen, J., and Sparks, J. P.: Modeling and measuring the effects of disturbance history and climate on carbon and water budgets in evergreen needleleaf forests, Agricultural and Forest Meteorology, 113, 185-222, 2002.

Tian, H., Chen, G., Zhang, C., Liu, M., Sun, G., Chappelka, A., Ren, W., Xu, X., Lu, C., Pan, S., Chen, H., Hui, D., Mcnulty, S., Lockaby, G., and Vance, E.: Century-Scale Responses of Ecosystem Carbon Storage and Flux to Multiple Environmental Changes in the Southern United States, Ecosystems, 15, 674-694, 2012.

Van Der Werf, G. R., Randerson, J. T., Giglio, L., Collatz, G. J., Mu, M., Kasibhatla, P. S., Morton, D. C., Defries, R. S., Jin, Y., and Van Leeuwen, T. T.: Global fire emissions and the contribution of deforestation, savanna, forest, agricultural, and peat fires (1997–2009), Atmos. Chem. Phys., 10, 11707-11735, 2010.

Vukićević, T., Braswell, B. H., and Schimel, D.: A diagnostic study of temperature controls on global terrestrial carbon exchange, Tellus B, 53, 150-170, 2001.

Wang, W., Ciais, P., Nemani, R. R., Canadell, J. G., Piao, S., Sitch, S., White, M. A., Hashimoto, H., Milesi, C., and Myneni, R. B.: Variations in atmospheric CO2 growth rates coupled with tropical temperature, Proceedings of the National Academy of Sciences, 110, 13061-13066, 2013.

Zeng, N., Mariotti, A., and Wetzel, P.: Terrestrial mechanisms of interannual CO2 variability, Global Biogeochemical Cycles, 19, GB1016, 2005.